ELSEVIER

Journal of Hazardous Materials 55 (1997) 1–22

JOURNAL OF HAZARDOUS MATERIALS

Effect of aqueous phase properties on clay particle zeta potential and electro-osmotic permeability: Implications for electro-kinetic soil remediation processes

Leland M. Vane *, Gwen M. Zang

National Risk Management Research Laboratory, US Environmental Protection Agency, Cincinnati, OH 45268, USA

Abstract

The influence of aqueous phase properties (pH, ionic strength and divalent metal ion concentration) on clay particle zeta potential and packed-bed electro-osmotic permeability was quantified. Although pH strongly altered the zeta potential of a Georgia kaolinite, it did not significantly change that of a Wyoming bentonite. The zeta potential for the kaolinite ranged from +0.7 mV at pH = 2 to −54 mV at pH = 10 (0.01 M KCl) while the bentonite zeta potential changed by only 5 mV (−31 to −36 mV) over the same pH range. For both clays, ionic strength was found to have a weak effect while divalent cations made the zeta potential markedly more positive. Charge reversal was observed for kaolinite at 100 ppm Pb^{2+} (pH = 5) with a background ionic strength of 0.01 M KCl and only 10 ppm Pb^{2+} with a background of 5×10^{-4} M KCl. A theoretical relationship between the electro-osmotic permeability coefficient for packed clay beds and particle zeta potential was developed and experimentally verified for kaolinite. For example, both the electro-osmotic permeability coefficient and particle zeta potential were found to be three times greater at pH = 5 than at pH = 3. As a result, rapid zeta potential analyses can be used to predict electro-osmotic performance for expected site conditions as well as to select electrolyte control strategies to optimize an electro-kinetic soil remediation process. © 1997 Elsevier Science B.V.

Keywords: Zeta potential; Kaolinite; Bentonite

* Corresponding author. E-mail: vane.leland@epamail.epa.gov

PII S0304-3894(97)00010-1

1. Introduction

The in situ remediation of a contaminated soil is an exercise in mass transfer limitations. The challenge is to mobilize the contaminant and transport it to a treatment/collection zone or to deliver nutrients, microorganisms, or destruction chemicals to degrade the contaminant where it resides. For soils with high hydraulic permeabilities, pressure driven hydraulic processes can be utilized to enhance the transfer of mobilization or treatment solutions into a contaminated zone. Mobilized contaminants and degradation products can be removed in the same manner. However, pressure driven hydraulic delivery/removal in low permeability soils ($k_h < 10^{-7}$ cm/s) is impractical.

One method of transporting solutions and compounds in low permeability soils is the application of an electric current to the soil. This form of remediation utilizes the response of charged molecules and particles to an applied voltage gradient to effect the movement of pollutants. Driving the remediation are the electro-kinetic phenomena of electro-osmosis, ion migration (electro-migration) and electrophoresis. As depicted in Fig. 1, most soil particles, including clays, carry a negative surface charge. When the soil is immersed in an electrolyte, the particles attract cations, creating a positively charged boundary layer (referred to as the charged double-layer) next to the surface of the soil particles. Application of a voltage difference across a section of soil causes movement of the ions and associated water within the double-layer toward the cathode (electron source). The remainder of the interparticle pore fluid moves in the same direction as the double-layer fluid due to viscous drag interactions. This net flow of pore fluid due to an applied voltage gradient is termed 'electro-osmosis'. Electro-osmosis can be utilized to remediate contaminated soils in situ by flushing out the pore fluid and contaminants (or to deliver nutrients, surfactants, etc.). The ions in the bulk pore fluid also respond to the applied voltage gradient, with the anions being driven to the anode and cations driven to the cathode. This movement of aqueous ions and ion-complexes in

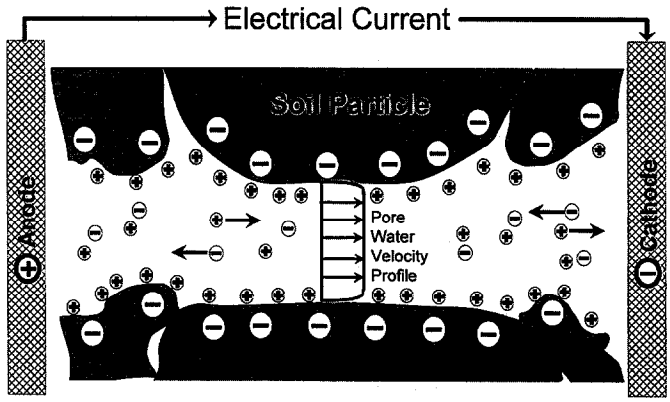

Fig. 1. Schematic illustration of electro-kinetic processes in a soil pore (adapted from [16]).

response to the voltage gradient is referred to as ion migration or electro-migration. Electro-migration can be used to recover ionic contaminants from soil, even in unsaturated soils [1]. Larger charged molecules and particles also move due to an applied voltage gradient (electrophoresis). Substances which fall into this latter category include cationic or anionic surfactant micelles, clay particles, microorganisms and poly-electrolytes.

Long used to dewater soils and sludges and to stabilize embankments [2–5], electro-kinetic processes are emerging as powerful tools to overcome the mass transfer challenges presented by contaminated low permeability soils [6–10]. Over the past decade, researchers have investigated the use of electro-kinetic processes to effect the movement of heavy metals, organics and nutrients in saturated low permeability clays and soils at bench, pilot and field scales with varying degrees of success. Investigations with more porous soils and unsaturated soils as well as efforts to model the processes have also been initiated [11–16]. The general application of electro-kinetics involves driving the contaminant from the soil to one of the electrodes where it would be collected or treated. Recently, a concept was proposed to place treatment zones between the electrodes, thereby reducing the distance the mobilized contaminant would have to travel before being removed/degraded and, concomitantly, reducing the time required to remediate a site. This layering of treatment zones between electrodes has been termed 'Lasagna Technology' by the developers [17–20].

All three of the aforementioned electro-kinetic phenomena (electro-osmosis, electro-migration and electrophoresis) will develop during an electro-kinetic soil remediation. The degree to which each process occurs depends on the properties of the soil/pore fluid matrix including the degree of saturation, ionic strength of pore fluid, types of ions/charged particles present, pH of pore fluid, temperature, porosity of soil, soil composition (% clay, type of clay, etc.) and the zeta potential (surface electrostatic potential) of the soil particles. In this paper, we will demonstrate the importance of aqueous phase properties (such as pH, ionic strength and divalent cation concentration) and clay type to particle zeta potential and relate this dependence to bench-scale electro-osmosis performance.

2. Theoretical background

As mentioned in Section 1, a charged particle immersed in an electrolyte will attract ions of opposite charge. The net charge in the charged double-layer surrounding the particle is approximately equal to that of the particle (although of opposite sign). When placed in an electric field, the particle will move by electrophoresis toward the oppositely charged electrode. The velocity of this particle (v_p) is dependent on the viscosity of the fluid (η), the applied voltage gradient (E), the zeta potential (ζ) of the particle and a shape function f_1 as described by the equation of Henry [21]:

$$v_p = \frac{2\varepsilon\zeta E}{3\eta} \cdot f_1(\kappa a) \tag{1}$$

where κ is the Debye-Hückel parameter, a is the radius of the particle and ε is the permittivity of the fluid. A negative particle velocity indicates movement toward the anode and a negative zeta potential. The distance $1/\kappa$ is referred to as the 'double layer thickness'. For an aqueous solution at 25°C, $\kappa = 3.29(I)^{1/2}$ (nm^{-1}) where I is the ionic strength, and $\varepsilon = 7.0 \times 10^{-10}$ farad/m [21]. Therefore, as the ionic strength of the solution increases, the double layer thickness decreases. The function f_1 in Eq. (1) ranges from 1 for small values of κa (i.e. small particles with relatively thick double layers) up to 1.5 for large κa values ($\kappa a > 100$, large particles with thin double layers). Therefore, for clay samples with an average particle radius of 1 μm in a 0.01 ionic strength aqueous solution, $\kappa a \approx 330$, $f_1 \approx 1.5$, and Eq. (1) reduces to Smoluchowski's classic equation [21]:

$$v_p = \frac{\varepsilon \zeta E}{\eta} \tag{2}$$

Similarly, when a packed bed of clay particles is saturated with an electrolyte and exposed to a voltage gradient, the electro-osmotic volumetric flow rate (q_{eo}) resulting from the movement of solvated ions concentrated outside the stationary layer is described by the Helmholtz-Smoluchowski equation (assuming $\kappa a > 100$) [11,12,21,22]:

$$q_{eo} = \left(\frac{-\varepsilon \zeta E}{\eta}\right)\left(\frac{An}{\tau^2}\right) \tag{3}$$

where A, τ and n are the total cross-sectional area, tortuosity and porosity of the sample, respectively. Tortuosity is defined as the ratio of the actual distance an average fluid particle travels to the straight-through distance in the direction of net transport. In Eq. (3), a negative zeta potential results in a positive flow rate, indicating flow toward the cathode. The similarity between Eqs. (2) and (3) is unmistakable. The first term in parentheses in Eq. (3) is equivalent to Eq. (2), describing the velocity of a particle in dilute suspension. The second term simply describes the structural properties of a packed bed of particles. The main difference between the two equations is simply the frame of reference: the reference point is fixed in the electrolyte volume in Eq. (2), but fixed on a particle in Eq. (3). Traditionally, Eq. (3) has been recast as [12,14,15,23]:

$$q_{eo} = k_{eo} EA \tag{4}$$

where k_{eo} is the electro-osmotic permeability coefficient with units of cm^2/V-s or cm^2/V-day defined by the following relationship:

$$k_{eo} = \left[\frac{-\varepsilon \zeta n}{\eta \tau^2}\right] \tag{5}$$

The zeta potential of most charged particles is dependent on solution pH, ionic strength, types of ionic species, temperature and type of clay minerals [12,22,24–34]. According to Eq. (3), the electro-osmotic flow rate observed in packed beds of charged

particles should also be a function of these same parameters. Investigators of electro-kinetic soil remediation processes have observed the development of often dramatic pH, conductivity, temperature and species concentration gradients [13,22,34–38]. The pH gradients arise from electrolysis reactions which occur at the powered electrodes (shown below for unreactive electrodes):

$$\begin{aligned} 2H_2O - 4e^- &\Rightarrow O_2 \Uparrow + 4H^+ \quad @\text{Anode} \\ 2H_2O + 2e^- &\Rightarrow H_2 \Uparrow + 2OH^- \quad @\text{Cathode} \end{aligned} \tag{6}$$

The anode region becomes acidic (pH as low as 2) while the cathode region is basic (pH as high as 12). As a result, the zeta potential may be highly position dependent. Unfortunately, models for the electro-kinetic processes have only recently included the zeta potential as a variable [12,22]. Shapiro and Probstein [22] incorporated ζ as a fitting parameter, constant over the entire sample, while Eykholt [12] used zeta potential literature values for kaolinite to introduce ζ as a function of pH. Jacobs et al. [11] mentioned incorporating the effect of pH, ionic concentrations and soil type on ζ in future versions of their model.

When electro-osmosis is relied upon to transport contaminants (as with uncharged contaminants with or without non-ionic surfactants), the time required to remediate a site is proportional to the electro-osmotic flow rate, assuming that the contaminant in the pore fluid is in equilibrium with the sorbed contaminants. Therefore, based on Eq. (3), variations in ζ and E directly impact the remediation time. Even when electro-migration is the desired transport process, the amount of electro-osmosis must be factored into the remediation plan. While E can be independently controlled at the electrodes, ζ is determined solely by the subsurface conditions which may be dramatically affected by the remediation process and may be a function of location in the soil. For this reason, it is critical that the zeta potential of the soil be evaluated based on the expected conditions during the remediation as well as based on depth and position at the site.

The zeta potentials of small particles in dilute suspensions have been routinely measured using instruments which range from relatively simplistic manually operated optical electrophoresis devices to more involved automated light scattering devices [21,27,33,39–48]. These instruments allow the rapid determination of zeta potential as a function of solution properties with a high degree of control over these properties. Therefore, a wide range of variables can be investigated in a reasonable amount of time. Conversely, bench-scale electro-osmosis experiments in compressed clay samples suffer from little control over variables such as pH, conductivity, and types of ionic species both as a function of position in the sample and of time. As a result, it is difficult to distill zeta potential information from long term electro-osmosis data, although this type of larger scale data is required to more fully evaluate the process under field conditions. Streaming potential determinations for packed soil samples represent another method for evaluating the impact of aqueous property changes on electro-kinetics [21]. This method falls between the extremes of bench-scale electro-osmosis experiments and dilute-suspension electrophoresis measurements in terms of time required and control over aqueous properties.

3. Experimental

3.1. Materials

Three clay materials were evaluated. The kaolinite (air-dried, air-floated Georgia kaolinite, Thiele Kaolin Company, Sandersville, Georgia) and bentonite (Bara-Kade, a Wyoming bentonite, Bentonite Corporation, Denver, Colorado) materials are described in Table 1. A silty–clay soil sample from Southwestern Ohio was also evaluated, but required more preparation due to the presence of larger particles. The silty–clay soil was prepared for zeta potential analysis by dispersing the sample in distilled water and allowing it to stand quiescent for 1 min. The top layer of the mixture was then poured off and dried. The particles which remained suspended in this top layer were referred to as the 'fine fraction' and represented approximately 50 wt.% of the initial soil sample. Zeta potential experiments were performed with only the fine fraction. No such separation was necessary for the kaolinite or bentonite materials.

All solutions were prepared with either house distilled water (< 2.0 μS/cm) or distilled deionized (DDI) water (< 0.7 μS/cm) and the following reagent grade salts (from Fisher Chemical, unless noted otherwise): $Pb(NO_3)_2$, $CaCl_2 \cdot 2H_2O$, KCl (Aldrich), $Cu(NO_3)_2 \cdot 3H_2O$ (Fluka), NaCl and $AlCl_3 \cdot 6H_2O$. In order to create uniform and reproducible clay samples for zeta potential analysis, the clays were pretreated with either 1 M KCl, 1 M HCl, or DDI water. Pretreated clays were prepared by dispersing 5 g of clay in 45 ml of treating solution and shaking for 5 h. Samples were then centrifuged at 3500 rpm, supernatant decanted, a second 45 ml of treating solution added, samples shaken for 20 h, centrifuged, and supernatant decanted again. The treating solution was rinsed from the samples by adding 45 ml of DDI water, shaking for 15–30 min, centrifuging, and decanting the water. This rinse procedure was repeated five times, followed by a 20 h rinse and a final 15–30 min rinse. The clays were dried in glass vials at 105°C for 24 h, capped, and stored in a vacuum desiccator. KCl-treated

Table 1
Properties of clay samples[a]

Property: method (units)	Kaolinite	Bentonite
Mineralogical composition: X-ray diffraction	92% Kaolin 8% Illite /Mica trace-Smectite	89% Montmorillonite 7% Quartz 3% Illite trace-Plagioclase
Specific gravity: ASTM D854	2.62 ± 0.02	2.770 ± 0.003
Cation exchange capacity: EPA 9081 (meq/100 g)	12.5 ± 2.8[b]	84.1 ± 0.7
Hydraulic permeability: ASTM D5084 (cm/s)	4×10^{-8}	$\approx 4 \times 10^{-10}$
BET surface area (m^2/g)	19.4 ± 0.1	27.6 ± 0.2
Proctor max. dry density: ASTM D698 (kg/m^3)	1338	N/A
Proctor optimum moisture: ASTM D698 (%)	31.0	N/A
Atterberg limits (liquid/plastic): ASTM D4318	62%/30%	N/A

[a] Analyses performed by IT Corporation Geotechnical Laboratory.
[b] The CEC of kaolinite from the same source has been reported to be 1.06 meq/100 g based on lead adsorption isotherms [37].

clays were used as the reference material for most of the zeta potential analyses while untreated kaolinite was used for bench-scale tests due to the large mass of material required.

3.2. Electrophoresis experiments

The effect of pH, ionic strength, clay type and ionic species on zeta potential was evaluated using an automated micro-electrophoresis instrument (ZetaSizer 4 with ZET5104 cell, Malvern). The instrument reports a zeta potential distribution, the mean of the distribution and the width of the distribution. In this procedure, 0.01 g clay was transferred to a 125 ml polypropylene bottle to which 100 ml of an aqueous solution and a magnetic stirring bar were subsequently added yielding a final clay concentration of 0.1 g/l. The clay was dispersed by stirring the sample while sparging with argon. The pH was measured with a combination electrode (Orion Ross #81-03 calibrated with pH = 4.00, 7.00 and 10.00 standards) and adjusted by dropwise addition of HCl or KOH solutions. All samples contained a minimum of 10^{-4} M KCl (generally 0.01 M) so pH adjustments would not alter the background ionic strength. After shaking overnight (20–24 h), pH was readjusted to the desired level, if necessary, before electrophoresis analysis. Before analyzing each set of samples, the optics of the ZetaSizer 4 were aligned and the quartz capillary was cleaned with ethanol, DDI water and a swab. The operation of the instrument was checked before and after each set of data by analyzing a fresh 0.1 g/l suspension of Minusil in DDI water. The zeta potential of Minusil is reported to be -29 mV [43]. Mean values of -29 ± 3 mV were accepted as an indication that the operation of the instrument was acceptable. Minusil values outside this range, multiple zeta potential peaks, or an overly broad peak required realignment of optics or more thorough cleaning of the capillary.

Two 10 ml sample aliquot replicates were injected into the cell and analyzed for sample zeta potential, the average of these readings was calculated and reported with the 'width' of the zeta potential peak as provided by the instrument. Duplicate suspensions of at least one sample per set were prepared to determine precision. In figures presented herein, the error bars represent the average width of the raw data peaks or the standard deviation of the means at a given pH or concentration, whichever was greater. The capillary was flushed between samples with an excess of DDI water to minimize sample carry-over.

3.3. Adsorption experiments

Adsorption isotherms for Pb^{2+}, Ca^{2+} and Cu^{2+} on kaolinite were separately determined in order to further investigate the response of the clay zeta potential to changes in concentrations of these cations. 5.0 g of kaolinite was weighed into 50 ml polypropylene centrifuge tubes to which 40 ml of a metal salt solution was added. The solutions ranged in cation concentration from 0–1000 mg/l. Background electrolyte of 0.01 M KCl and pH = 4 (3.8–4.2) was maintained in all samples. A second Pb^{2+} adsorption series was performed with a background electrolyte of 0.0005 M KCl, also at pH = 4. Duplicate clay samples and one blank (no clay) were prepared at each metal ion

concentration. Samples were shaken at room temperature (23°C) for 24 h then centrifuged at 3500 rpm for 15 min. Sample pH was measured, if the pH was not in the range 3.8–4.2, the pH was adjusted and samples shaken for another 24 h. This procedure was repeated until the sample pH stabilized, at which time the supernatant was transferred to 15 ml centrifuge tubes for analysis.

The metal ion concentration in the supernatant was determined by direct aspiration flame atomic absorption spectrophotometry (Perkin Elmer 3100). If necessary, samples were diluted prior to analysis with aliquots of background electrolyte to maintain constant background electrolyte levels. Standards were also prepared with 0.01 M KCl background electrolyte. Recovery levels for analysis matrix spike samples were acceptable (> 90%) for all metals. The metal loading on the clay (reported as mg-metal/g-clay) was calculated using the following relationship: loading = (0.04 l) (mg-metal/l in No Clay Blank − mg-metal/l in clay sample)/(mass of clay). To ensure that this relationship truly represented the metal loading, six Pb^{2+} samples with an average equilibrium Pb^{2+} concentration of 2.1 ± 0.2 mg/l were extracted with 1.6 M HNO_3. The loading calculated using the above relationship was within 2% of the loading calculated from the amount of lead extracted (0.060 ± 0.002 vs. 0.059 ± 0.002 mg-Pb/g-clay).

3.4. Electro-osmosis experiments

Electro-osmosis experiments were performed in an apparatus similar to those used by other investigators [28,36,37,49]. A schematic diagram of the apparatus described herein is presented in Fig. 2. The sample cell consisted of a 7.62 cm ID acrylic tube ($A = 45.6$

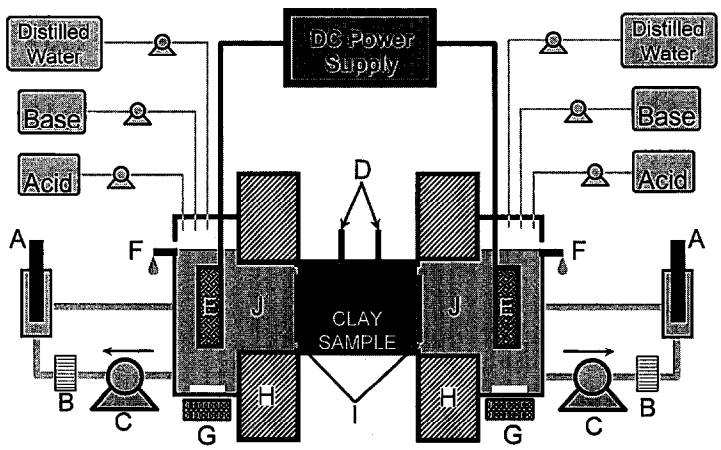

Fig. 2. Schematic diagram of bench-scale electro-kinetics apparatus (argon purge not shown). (A) pH probe; (B) conductivity probe; (C) electrolyte recirculation pump; (D) platinum sensing electrode; (E) platinum mesh powered electrode; (F) overflow weir (to overflow bottle); (G) magnetic stirrer; (H) end plate (cross-sectioned); (I) sensing electrode and acrylic disc and (J) electrolyte.

cm^2). To prepare the sample, an aqueous solution/clay slurry (60–75 wt.% water) was mixed for over 24 h in a reciprocating shaker. The slurry was poured into a vertically oriented sample cell (bottom spanned by nylon filters and a platinum mesh sensing electrode stretched over a perforated acrylic disk). Once poured, the slurry was gently stirred to remove air bubbles. A perforated acrylic disk covered by nylon filters was inserted into the top of the sample cell. The cell was then placed between two end plates held together by threaded rods. A hand operated compaction screw was used to exert 90.7 kg of force (approximately 200 kPa) on the top disk. The force was applied until no additional movement in the compaction screw was observed, which generally required 2–3 weeks. Over this time, sufficient water was expressed from the sample to yield a 32 ± 2 wt.% water sample. The moisture content of the clays was determined using a standard gravimetric method [50]. The cell was removed from the compaction mold, the top acrylic disk removed, excess clay removed, and a second platinum mesh electrode/nylon filter/acrylic disk assembly inserted into the open end. The second electrode assembly was pressed into place using the compaction screw. The cell was then placed between a second set of end plates equipped with electrolyte reservoirs.

The electrolyte in each of the end plate reservoirs was circulated through a conductivity probe (Cole-Parmer #19500-30) attached to a controller (Cole-Parmer #19300-00) and a pH probe assembly (Orion #81-03 Ross combination electrode with KCl reference solution) also attached to a controller (Cole-Parmer ChemCadet). The electrolyte pH was controlled by addition of 0.05 M KOH at the anode and 0.05 M HCl at the cathode. Since the neutralization of electrolysis products yielded an increase in the ionic strength of the electrolyte, conductivity could be controlled by the addition of distilled water. Peristaltic pumps (Cole-Parmer Masterflex pumps with Pharmed tubing) were used for all fluid delivery and circulation applications. A constant level in the reservoirs was maintained by a weir-type overflow port. Overflow electrolyte was collected in 4 l polypropylene bottles. Humidified argon was sparged into both reservoirs to remove hydrolysis gases (O_2 or Cl_2 at the anode and H_2 at the cathode) and to keep CO_2 out of the system. To determine the amount of water transported by electro-osmosis, the acid, base, DI water and overflow bottles were weighed every 1 to 3 days. The net outflow from the anode reservoir was averaged with the net inflow to the cathode reservoir and normalized for a 24 h period to yield a daily electro-osmotic flow (g/day). 'Blank' electro-osmosis measurements were made with zero current to ensure that no leaks existed and to verify that no flow occurred without an applied current.

A constant current of 5.0, 10.0 or 20.0 mA (Hoefer Scientific PS500X power supply, modified to operate in 0–40 mA range with 0.1 mA readability) was applied via platinum mesh electrodes immersed in the electrolyte at the end plate reservoirs. The actual current was determined by measuring the voltage across a 100 ohm resistor in series with the sample. Voltages were measured with a multimeter (Keithley model #197A) using the platinum mesh sensing electrodes located on the clay side of the perforated acrylic disks and 16 mm diameter platinum rods inserted into the clay through 32 mm NPT compression fittings located along the length of the sample. Voltages were corrected for the zero current electrode voltages measured when the power supply was turned off. The voltage gradient across the sample (E_{cell}) was time

averaged between electro-osmosis readings and used to calculate the electro-osmotic permeability coefficient:

$$k_{eo} = \frac{q_{eo}}{E_{cell} A} \tag{7}$$

The pH of the clay in the cell was determined by inserting a spear tip combination pH probe (Orion #81-63) into the sample through the 32 mm NPT holes where voltages were measured, and recording the pH after it had stabilized. The pH probe was calibrated before each set of measurements and between each sample port with pH = 7.00 and 4.00 standards. Probe calibration was checked after each sample and the probe tip and ceramic junction were thoroughly cleaned between samples.

A new experiment was initiated by changing the electrolyte pH and conductivity set points. Each experiment was continued until k_{eo} and the clay pH reached constant values. This process took from 3 to 8 weeks for the 10.16 cm sample and 2 to 4 weeks for the 2.54 cm sample. The series of clay pH values investigated over the course of 9 months for the 10.16 cm sample was (in chronological order): 2.5, 4.4, 4.6, 4.8, 4.9 and 2.8 (all with 0.01 M KCl). The chronological series of clay pH values investigated over the course of 5 months for the 2.54 cm sample was (all with 0.01 M KCl unless otherwise noted): 4.6 (0.0035 M KCl), 4.7, 5.65, 5.9, 4.8, 2.8 and 4.2. After this series of pH, the impact of calcium ions on the performance of the 2.54 cm bench sample was investigated by continuously adding a 100 mg/l calcium solution (calcium chloride dissolved in acidified DDI water) to the 400 ml electrolyte reservoirs at a rate of 1.2 l/day. An electrolyte pH of 4.2 and background of 0.01 M KCl were maintained.

Each completed series of pH/conductivity values was followed by removal of the cell from the end plates and removal of the intact sample. The 10.16 cm sample was divided into four 2.54 cm sections. The 2.54 cm sample was not divided except for duplicate sampling. Two clay pH measurements and two moisture analyses were performed per section (as described above). Two portions of the 2.54 cm sample were placed in 50 ml centrifuge tubes containing 1.6 M HNO_3 followed by Flame-AA analysis for extracted calcium. Based on this analysis and the calcium adsorption isotherm for this kaolinite, the calcium concentration in the pore fluid was estimated to be 10 ppm.

4. Results and discussion

The effect of pH on the zeta potential of kaolinite, bentonite and silty–clay soil samples is presented in Fig. 3. The zeta potential of kaolinite was found to be a strong function of pH, ranging from +0.7 mV at pH = 2.0 to −54 mV at pH = 10.0. Untreated, DDI water-treated, HCl-treated and KCl-treated kaolinite samples all exhibited the same behavior and the respective results were, generally, within experimental error. This similarity between the four kaolinite data sets presented in Fig. 3 indicates that the method of pretreating the samples did not affect the measured zeta potential. It is also apparent from Fig. 3 that the behavior of bentonite in response to pH changes

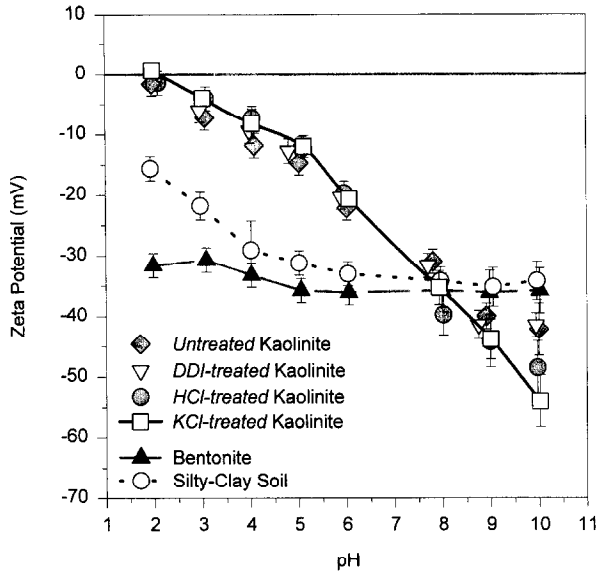

Fig. 3. Effect of pH on zeta potential of kaolinite, bentonite and silty–clay soil samples. All samples: 0.1 g-clay/l suspensions in 0.01 M KCl at 25°C.

was markedly different than that of kaolinite. In fact, the zeta potential of bentonite did not change by more than 20% over a pH range of 2–10 (−31 to −36 mV). Over most of this pH range, the zeta potential of bentonite was found to be more negative than that of kaolinite. The silty–clay soil displayed a response intermediate to that of the kaolinite and bentonite samples.

Although zeta potential studies have been performed with kaolinite [33,39,42,43,45–48] and bentonite [21,27,40–43] in the past, the source of clay, method of preparation, and composition of the aqueous solution are rarely the same between references and often unreported or uncontrolled. Within these constraints, however, there is good agreement between the data shown in Fig. 3 and the literature data. The general shapes of ζ vs. pH curves in the literature are similar to those in the figure, while the main differences are in the low pH region. For example, the average kaolinite zeta potential from this work and several references [43,45,46,48] is -9 ± 14, -34 ± 5 and -46 ± 2 mV at pH 4, 7 and 10, respectively (all at approximately 0.001 M ionic strength). The large standard deviation at pH = 4 is likely due to differences in clay preparation as well as the effect of increasing acid concentration on the ionic strength (since the H_3O+ and A^- concentrations are approaching that of the background ions). For bentonite, data from this work and several references [21,40,43] indicate that the zeta potential is relatively insensitive to pH with an average zeta potential of -30 ± 4 mV (with approximately 0.001 M ionic strength).

As was the case with pH, kaolinite exhibited a more pronounced sensitivity to background electrolyte concentration than did bentonite, as illustrated in Fig. 4 at constant pH in KCl solutions. These results are consistent with observations from the

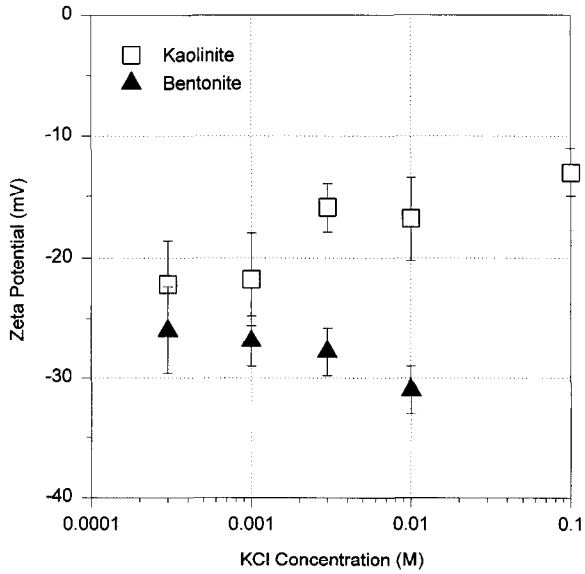

Fig. 4. Variation of zeta potential with electrolyte concentration for kaolinite and bentonite at constant pH. All samples: KCl-treated, 0.1 g-clay/l suspensions in KCl solutions at 25°C and pH = 5.9 ± 0.2.

literature [21,40,44,46], again, within the constraints of the literature measurements performed. For example, Delgado et al. [40] also found that the zeta potential of bentonite was relatively insensitive to NaCl concentration. Others have found that the zeta potential of bentonite, though relatively constant at -30 mV between 10^{-5} and 10^{-2} M, did fluctuate up to 10 mV with changes in the concentration of indifferent electrolyte [21].

This dependence of zeta potential on background electrolyte concentration is, itself, a function of pH as illustrated in Fig. 5 for kaolinite. Over most of the pH range (4–10), the magnitude of ζ is decreased as the KCl concentration increases. This trend disappears and may even be reversed below pH = 4. Williams and Williams [46] made a similar observation for kaolinite suspended in NaCl solutions with a trend reversal at pH = 5.

Although the zeta potential of bentonite was not a strong function of pH or KCl concentration, it did respond markedly to the presence of Pb^{2+} ions as shown in Fig. 6. The magnitude of the zeta potential was reduced from 33 to 10 mV by the introduction of 1000 mg/l Pb^{2+} at pH = 5 and 0.01 M KCl. Also shown in Fig. 6 is the effect of increasing levels of Pb^{2+}, Cu^{2+} and Ca^{2+} on the zeta potential of kaolinite at pH = 4.0. For each of these metal ions, the sign of the kaolinite zeta potential is reversed at approximately 100 mg-cation/l when 0.01 M KCl is present in the background. Dramatic reductions in the magnitude of bentonite zeta potential (asymptotic approach to zero) due to increases in calcium concentration and zeta potential sign reversal for modest levels of aluminum and thorium have been reported [40]. Aluminum (added as alum) was also found to reverse the sign of zeta potential for kaolinite [42]. Many

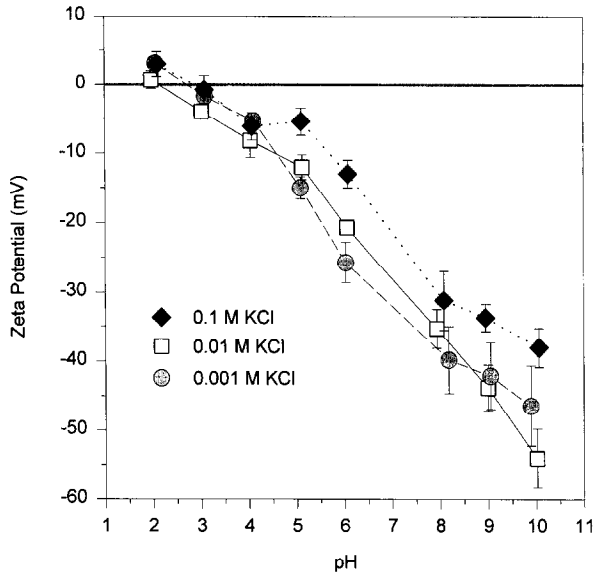

Fig. 5. Effect of electrolyte concentration on the relationship between zeta potential and pH for kaolinite. All samples: KCl-treated, 0.1 g-clay/l suspensions in KCl solution at 25°C.

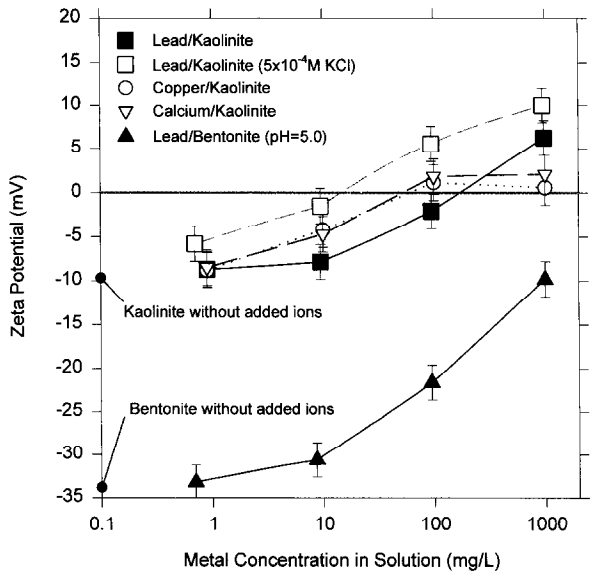

Fig. 6. Influence of divalent cation concentration on kaolinite and bentonite zeta potential. Legend indicates divalent cation and clay represented by data. Samples: 0.1 g-clay/l suspension, 25°C, 0.01 M KCl and pH = 4.0, unless otherwise noted.

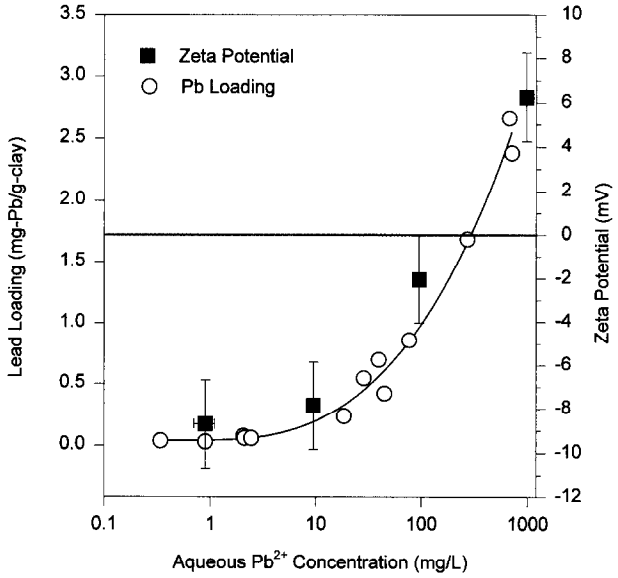

Fig. 7. Relationship between lead loading and aqueous lead concentration and between kaolinite zeta potential and aqueous lead concentration. All samples: untreated kaolinite, pH = 4.0, 0.01 M KCl, 25°C; zeta potential samples: 0.1 g-clay/l suspensions; adsorption samples: 5.0 g-clay/40 ml $Pb(NO_3)_2$ solutions.

examples of the impact of potential determining ions, such as aluminum and cationic poly-electrolytes, and indifferent ions, such as sodium, on the zeta potential of particles have been reported [24,26,29–31,43]. Theoretically, zeta potential charge reversal should result in a reversal of the direction of electro-osmotic flow.

To investigate the effect of reduced background ion concentration on the response of zeta potential to increasing levels of divalent cations, the lead–kaolinite series first performed with a background of 0.01 M KCl was repeated with only 5×10^{-4} M KCl present. As displayed in Fig. 6, the 5×10^{-4} M KCl lead-zeta potential data (open squares) are measurably more positive than the 0.01 M KCl data (solid squares). This can be quantified by noting the Pb^{2+} concentration required to achieve a zero zeta potential. Approximately 10 mg/l Pb^{2+} is required when in the presence of 5×10^{-4} M KCl while over 100 mg/l Pb^{2+} is necessary to reverse the sign of kaolinite suspended in 0.01 M KCl. These results suggest that lead ions are better able to compete for sorption sites when fewer potassium ions are present. Lead adsorption experiments performed for this study confirmed that more lead was adsorbed at the lower KCl concentration. Furthermore, the amount of lead sorbed correlated with zeta potential for kaolinite as shown in Fig. 7. A similar behavior was observed for Cu^{2+} and Ca^{2+} at concentrations less than 100 mg/l. However, between 100 and 1000 mg/l, the amount of Cu^{2+} and Ca^{2+} adsorbed increased while the zeta potential remained essentially unchanged at about 0 to 2 mV. This zeta potential behavior (asymptotic approach to zero zeta potential) is similar to that observed in the presence of an indifferent electrolyte, while the strong reversal of the zeta potential charge observed for Pb^{2+} is typical of a specifically adsorbed/potential determining ion [21].

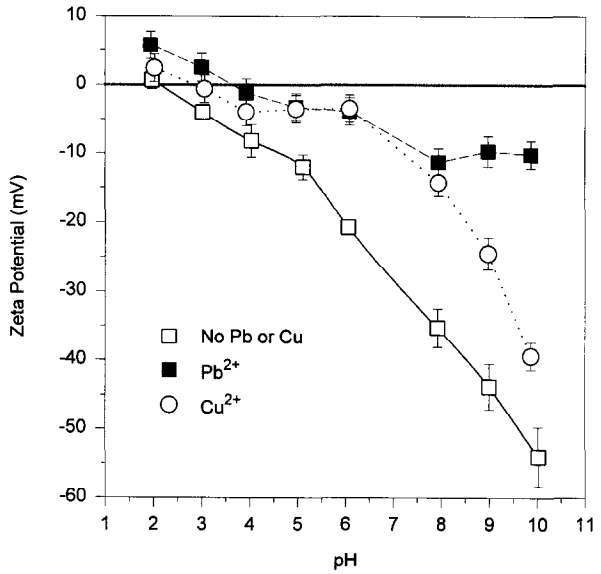

Fig. 8. Effect of aqueous Pb(II) and Cu(II) ions on the relationship between zeta potential and pH for kaolinite. Samples: KCl-treated kaolinite, 0.1 g-clay/l suspension, 0.01 M KCl, 10^{-4} M $Pb(NO_3)_2$ or $Cu(NO_3)_2$, and 25°C.

The data presented in Fig. 6 were all measured at constant pH. Since it has been observed that pH alters the impact of potential determining ions on particle zeta potential [29,43], the effect of pH on kaolinite zeta potential in the presence of 10^{-4} M Pb^{2+} (20.7 mg/l) and, separately, 10^{-4} M Cu^{2+} (6.4 mg/l) was also studied. As presented in Fig. 8, over the entire pH range studied, the presence of Pb^{2+} or Cu^{2+} resulted in a more positive zeta potential. The deviations were most pronounced for pH values greater than 5 and likely result from the pH-dependent sorption and speciation behavior of these hydrolyzable metals on the kaolinite.

The results presented in Figs. 3–8 illustrate the complex relationship between clay particle zeta potential and aqueous phase properties. These results highlight the importance of understanding the pore fluid chemistry of a field site and the impact of remediation efforts on that chemistry. As suggested by Eq. (3), this sensitivity of clay particle zeta potential to aqueous phase properties translates into a sensitivity of the electro-osmotic flow rate in a porous clay zone to the properties of the pore fluid. Bench-scale electro-osmosis experiments with kaolinite samples were performed to elucidate the sensitivity of the electro-osmotic flow rate to changes in pore fluid pH and conductivity. Bench-scale data are reported in terms of k_{eo} which can be related to ζ using Eq. (5).

As indicated by the zeta potential results and Eq. (5), k_{eo} for a packed porous bed of kaolinite should be a strong function of pH and divalent ion concentration, but weakly dependent on background ionic strength (as KCl). Furthermore, according to Eq. (5), operational parameters such as applied current/voltage gradient and polarity of the

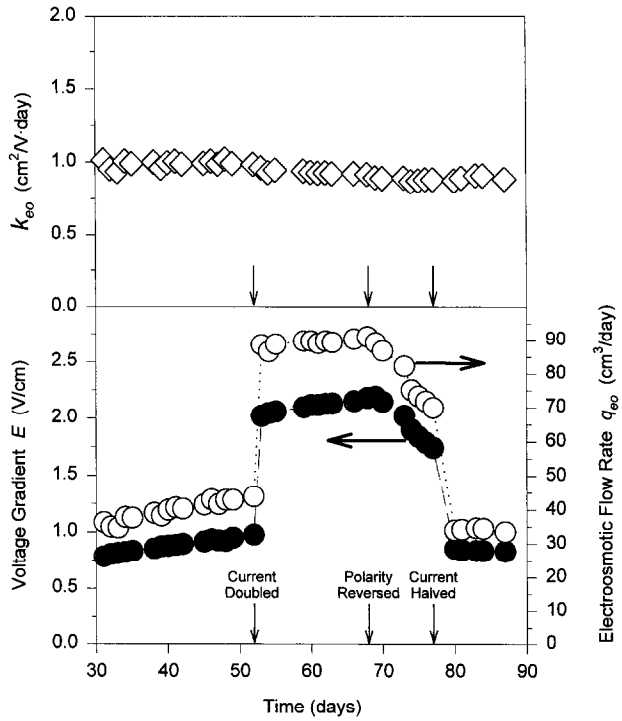

Fig. 9. Time dependence of cell voltage gradient and electro-osmotic flow rate (bottom graph) and electro-osmotic permeability coefficient (top graph) for bench-scale sample. Kaolinite sample is 10.16 cm long, initial current = 10.0 mA.

electrodes (direction of current flow) should not impact k_{eo} unless sample heating or swelling/shrinking of the clay occurs. This predicted insensitivity is borne out by the experimental data presented in Fig. 9. The bottom graph in Fig. 9 displays the measured E_{cell} and q_{eo} values for the 10.16 cm long bench-scale sample while the k_{eo} values calculated from these quantities are plotted in the top graph, all as a function of time. As noted in the figure, the applied current was doubled on day 52, polarity reversed on day 68, and current halved (returned to original current) on day 77. E_{cell} and q_{eo} were significantly impacted by these operational adjustments. For example, both quantities exhibited a two fold increase after the current was doubled at day 52. As predicted, however, k_{eo} was not affected by these adjustments, changing by less than 2% between the days immediately before and after an adjustment and by less than 10% over the entire time frame displayed in Fig. 9 (60 days).

The variations of k_{eo} with clay pH for the 2.54 cm and 10.16 cm bench-scale samples are presented in Fig. 10. In addition, the solid circles in Fig. 10 represent the values of k_{eo} calculated using Eq. (5) (with $n = 0.55$ and $\tau = 1.25$) and the KCl-treated kaolinite ζ data from Fig. 3. Results from the 10.16 cm sample are in good agreement with k_{eo} values estimated from ζ data. However, k_{eo} values for the 2.54 cm sample are lower than for the 10.16 cm sample and ζ data. It was observed during the bench-scale

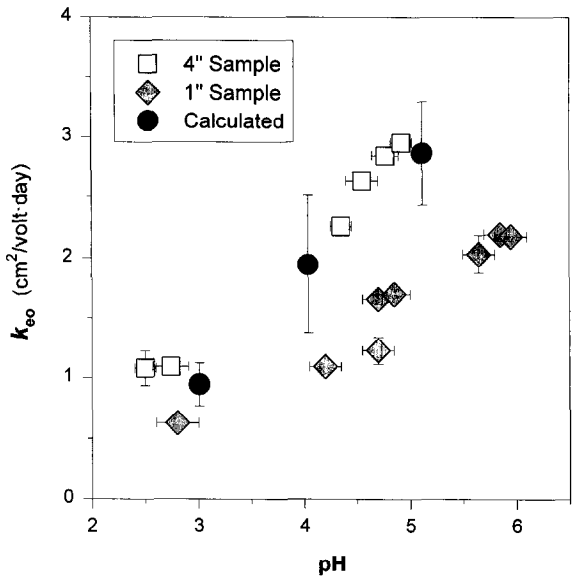

Fig. 10. Measured and calculated electro-osmotic permeability coefficients as functions of pH. Calculated values are based on the KCl-treated kaolinite zeta potentials presented in Fig. 3 and Eq. (5) with $n = 0.55$ and $\tau = 1.25$.

experiments that end effects caused by the transition from the aqueous solution to the porous media, restricted passage through the perforated acrylic disk, and presence of the nylon membrane filter between the sensing electrode and the clay resulted in a higher measured voltage gradient at the very ends of the clay sample than at the center of the sample. These end effects were present in both the 2.54 cm and 10.16 cm samples, but had more of an impact in the 2.54 cm sample. In both cases, it is believed that the voltage gradient used to calculate k_{eo} was artificially high, more so for the 2.54 cm sample. The net result is an underestimation of the actual k_{eo} values.

Although the values of k_{eo} for the bench-samples and from ζ data are not in exact quantitative agreement, it is apparent that they all follow the same trend with respect to pH. The benefit of the zeta potential measurements is not whether exact electro-osmosis values can be calculated, but whether the simpler dilute suspension experiments can predict trends and effects of ions and conditions on packed bed electro-osmosis. In this respect, the zeta potential measurements do very well. The best way to illustrate this capability is to normalize each data set in Fig. 10 by the pH = 4.0 data point of that set (determined from linear least squares fit of data). Normalizing the data in this manner should minimize biases associated with a particular bench-scale configuration and remove the influence of assumptions for tortuosity and porosity. The normalized k_{eo} and ζ data sets should fall on the same line since, from Eq. (5):

$$\frac{k_{eo}}{k_{eo(pH=4)}} = \frac{\zeta}{\zeta_{(pH=4)}} \tag{8}$$

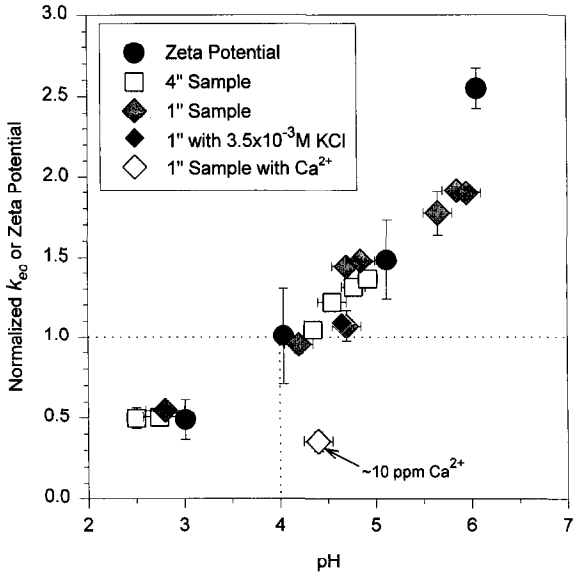

Fig. 11. Comparison of normalized electro-osmotic permeability coefficients and zeta potentials for kaolinite samples. All data are obtained with 0.01 M KCl unless otherwise noted; each data set is normalized by the data point at pH = 4.0 as determined from linear least squares fit of data.

As predicted, the data sets collapse onto the same line, as shown in Fig. 11. In all cases, the normalized value at pH = 5 is three times the normalized value at pH = 3, indicating that dilute suspension ζ data was capable of predicting the response of the electro-osmotic permeability of a bench-scale, packed bed of kaolinite to changes in pH. If the zeta potential and electro-osmosis data sets did not follow the same trend, then the normalized data sets would still intersect at pH 4 in Fig. 11, but would have different slopes.

Two other data points of interest are included in Fig. 11. First, as described in Section 3, the initial experiment performed with the 2.54 cm bench sample was with only 0.0035 M KCl electrolyte instead of the standard 0.01 M KCl used for the remainder of the bench experiments. In this case, the voltage gradient was approximately three times greater than with 0.01 M KCl. However, the electro-osmotic flow rate was also three times greater. As a result, the calculated k_{eo} was unaffected by electrolyte ionic strength. As shown in Fig. 11, the 0.0035 M KCl data point (solid black diamond) overlaps the 0.01 M KCl data point (gray diamond) which was obtained next in the sequence of experiments. This agrees with the observation from Fig. 4 that the zeta potential of kaolinite is not very sensitive to changes in KCl concentration, especially a 3-fold concentration change. Secondly, the final experiment with the 2.54 cm bench sample involved the addition of calcium ions to the electrolyte reservoirs (the estimated pore fluid Ca^{2+} concentration was 10 ppm). The resulting k_{eo} (white diamond in Fig. 11) was approximately one-third of the value for the preceding experiment in which calcium ions were not added (comparable KCl concentration and pH). The zeta potential data from Fig. 6 shows that the zeta potential of kaolinite drops by about 50% upon the

addition of 10 ppm Ca^{2+} at pH = 4. The agreement between the 67% reduction in k_{eo} observed for the 2.54 cm bench-scale sample and the 50% reduction in ζ for the dilute suspension micro-electrophoresis sample upon addition of 10 ppm is quite good considering that the pore fluid Ca^{2+} concentration of 10 ppm is an approximation.

Although this work has verified the relationship between zeta potential and electro-osmotic flow rate for kaolinite, additional work is required to establish the breadth of applicability of zeta potential analysis. For example, it remains to be seen if the electro-osmotic flow rate in a packed bentonite bed is insensitive to pH, as predicted by zeta potential data. Furthermore, real soils must be included to ensure that this analysis is applicable to heterogeneous samples as well as homogeneous clay samples.

5. Conclusions

This work quantified the sensitivity of clay particle zeta potential to clay type, pH, ionic strength and multivalent ionic species. The zeta potential of kaolinite was strongly dependent on pH and concentration of Cu^{2+}, Pb^{2+} and Ca^{2+} while only weakly dependent on background ionic strength (as KCl). Bentonite zeta potential was also a strong function of divalent metal ion concentration, but a weak function of pH and KCl concentration. Theoretical equations developed to describe electro-osmosis in porous clay beds predict k_{eo} to be a linear function of zeta potential, but independent of applied current and electrode polarity. Bench-scale experiments performed on saturated packed kaolinite samples verified this theoretical relationship — the response of bench-scale k_{eo} to pH, KCl and Ca^{2+} mirrored that of the dilute-suspension zeta potential data. As a result, the sensitivity of dilute suspension zeta potential to changes in aqueous phase properties can be used to predict the sensitivity of packed bed k_{eo} to changes in pore fluid properties. Since zeta potential measurements are significantly easier and faster to obtain than bench-scale k_{eo} measurements, a wider range of conditions can be manageably investigated. Understanding the influence of pore fluid chemistry on soil particle zeta potential and, by extension, electro-osmotic permeability, will lead to a more effective strategy for implementing electro-kinetic soil remediation processes. For example, electro-osmotic permeability could be increased by the informed selection of electrolyte conditions at the electrodes (such as low ionic strength, higher pH, low divalent cation concentration). Finally, it should be evident that past assumptions of constant or only pH-dependent k_{eo} for purposes of modeling electro-kinetic soil remediation processes are not accurate for situations where the electro-osmotic contribution to contaminant mass transport is significant and aqueous/clay properties are variable.

6. Disclaimer

This article has not been subjected to internal review by the US Environmental Protection Agency. As a result, the research results presented herein do not, necessarily, reflect agency policy.

7. Nomenclature

a	Particle radius [L]
A	Cross-sectional area [L^2]
E	Voltage gradient [V/L]
E_{cell}	Cell voltage gradient [V/L]
k_{eo}	Electro-osmotic permeability coefficient [$L^2V^{-1}\theta^{-1}$]
k_h	Hydraulic permeability [$L\theta^{-1}$]
n	Porosity [L^3/L^3]
q_{eo}	Electro-osmotic flow rate [L^3/θ]
ζ	Zeta potential [V]
η	Viscosity [$ML^{-1}\theta^{-1}$]
κ	Debye-Hückel parameter [1/L]
v_p	Particle velocity [$L\theta^{-1}$]
τ	Tortuosity [L/L]
ε	Permittivity [Farad/L]

Acknowledgements

The authors wish to thank Kim Fox (EPA) for the kind use of the zeta potential instrument, past/present members of the EPA Lasagna Team (Mike Roulier, Wendy Davis-Hoover, Taras Bryndzia, Jon Herrmann) for their support, and Steve Vesper of the University of Cincinnati for providing the silty–clay soil sample.

References

[1] EPRI Workshop, In-situ electrochemical soil and water remediation, February 28–March 1, 1994, Palo Alto, CA.
[2] I.W. Johnston, M.I.E. Aust, R. Butterfield, A laboratory investigation of soil consolidation by electro-osmosis, Aust. Geomech. J. G7 (1977) 21–32.
[3] L. Casagrande, Stabilization of soils by means of electro-osmosis state-of-the-art, J. Boston Society of Civil Engineers Section, ASCE 69 (2) (1983) 255–302.
[4] D.J. Kelsh, R.H. Sprute, Dewatering fine particle waste suspensions with direct current, in: Encyclopedia of Fluid Mechanics, ch. 27, Gulf Publishing, Houston, TX, 1986.
[5] N.C. Lockhart, Electro-osmotic dewatering of fine tailings from mineral processing, Int. J. Miner. Process. 10 (1983) 131–140.
[6] R.F. Probstein, P.C. Renaud, A.P. Shapiro, Electroosmosis techniques for removing hazardous materials from soil, US Patent No. 5.074.986, Dec. 24, 1991.
[7] Y.B. Acar, Electrokinetic cleanups , Civil Eng. October (1992) 58–60.
[8] Y.B. Acar, R.J. Gale, Electrochemical decontamination of soils and slurries, US Patent No. 5.137.608, August 11, 1992, Commissioner of Patent and Trademarks, Washington, DC, 1992.
[9] R.F. Probstein, R.E. Hicks, Removal of contaminants from soils by electric fields, Science 260 (1993) 498–503.
[10] R. Lageman, W. Pool, G. Seffinga, Electro-reclamation: theory and practice, Chem. Ind. 18 (1989) 585–590.

[11] R.A. Jacobs, M.Z. Sengun, R.E. Hicks, R.F. Probstein, Model and experiments on soil remediation by electric fields, J. Environ. Sci. Health A 29 (1994) 1933–1955.
[12] G.R. Eykholt, Driving and complicating features of the electrokinetic treatment of contaminated soils, Ph.D. dissertation, University of Texas, Austin, 1992.
[13] Y.B. Acar, R.J. Gale, G.A. Putnam, J. Hamed, R.L. Wong, Electrochemical processing of soils: Theory of pH gradient development by diffusion, migration, and linear convection, J. Environ. Sci. Health A 25 (1990) 687–714.
[14] A.N. Alshawabkeh, Theoretical and experimental modeling of multi species transport in soils under electric fields, Ph.D. dissertation, Louisiana State University, 1994.
[15] Y.B. Acar, A.N. Alshawabkeh, R.J. Gale, Fundamentals of extracting species from soils by electrokinetics, Waste Management 13 (1993) 141–151.
[16] A.P. Shapiro, P.C. Renaud, R.F. Probstein, Preliminary studies on the removal of chemical species from saturated porous media by electroosmosis, PCH PhysicoChemical Hydrodynamics 11 (1989) 785–802.
[17] C. Athmer, S.V. Ho, P.W. Sheridan, Laboratory study of the movement of trichloroethylene through clayey soils by electroosmosis, paper presented at 87th Annual Meeting of the Air and Waste Management Association, Cincinnati, OH, June 19-24, 1994.
[18] J. Trombly, Electrochemical remediation: Takes to the field, Environ. Sci. Technol. 28 (1994) A289–A291.
[19] 'Lasagna' Process Treats Contaminants, Environ. Protect., September 1994, 69-71.
[20] New Processes Promise To Enhance Soil Cleanup, Chem. Eng. Pro., April 1994.
[21] R.J. Hunter, Zeta Potential in Colloid Science: Principles and Applications, Academic Press, London, 1981.
[22] A.P. Shapiro, R.F. Probstein, Removal of contaminants from saturated clay by electroosmosis, Environ. Sci. Technol. 27 (1993) 283–291.
[23] A. Ugaz, S. Puppala, R.J. Gale, Y.B. Acar, Complicating features of electrokinetic remediation of soils and slurries: Saturation effects and the role of the cathode electrolysis, Chem. Eng. Comm. 129 (1994) 183–200.
[24] C.M. Cerda, K. Non-Chhom, The use of sinusoidal streaming flow measurements to determine the electrokinetic properties of porous media, Colloids Surfaces 35 (1989) 7–15.
[25] W.R. Bowen, R.A. Clark, Electro-osmosis at microporous membranes and the determination of zeta-potential, J. Colloid Interface Sci. 97 (1984) 401–409.
[26] S.K. Bhattacharjya, V.S. Gupta, B.K. Dutta, Industrial application of zeta potential studies: Effect of cationic polyelectrolytes on destabilization of clay colloids in synthetic waters, Fert. Technol. 12 (1975) 306–311.
[27] Y.S. Lee, J. Ree, T. Ree, Effect of zeta-potential on the viscosity of clay–water suspension, Bull. Korean Chem. Soc. 3 (1982) 83–88.
[28] R.E. Hicks, S. Tondorf, Electrorestoration of metal contaminated soils, Environ. Sci. Technol. 28 (1994) 2203–2210.
[29] Z. Sadowski, R.W. Smith, Effect of metal ions on the stability and zeta potential of barite suspensions, Miner. Metall. Proc. 4 (1987) 114–117.
[30] M.S. Celik, E. Yasar, Electrokinetic properties of some hydrated boron minerals, J. Colloid Interface Sci. 173 (1995) 181–185.
[31] J.M.W. Mackenzie, Zeta-potential studies in mineral processing: Measurement, techniques, and applications, Miner. Sci. Eng. 3 (1971) 25–43.
[32] Y.B. Acar, A.N. Alshawabkeh, R.J. Gale, A review of fundamentals of removing contaminants from soils by electrokinetic soil processing, Proceedings Mediterranean Conference on Environmental Geotechnology, May 25-27, 1992.
[33] G. Atesok, P. Somasundaran, L.J. Morgan, Charge effects in the adsorption of polyacrylamides on sodium kaolinite and its flocculation, Powder Technol. 54 (1988) 77–83.
[34] Y.B. Acar, A.N. Alshawabkeh, Principles of electrokinetic remediation, Environ. Sci. Technol. 27 (1993) 2638–2647.
[35] Y.B. Acar, J.T. Hamed, A.N. Alshawabkeh, R.J. Gale, Removal of Cd(II) from saturated kaolinite by the application of electrical current, Geotechnique 44 (1994) 239–254.
[36] Y.B. Acar, R.J. Gale, A.N. Alshawabkeh, R.E. Marks, S. Puppala, M. Bricka, R. Parker, Electrokinetic remediation: Basic principles and technology status, Hazard. Mater. 40 (1995) 117–137.

[37] J. Hamed, Y.B. Acar, R.J. Gale, Pb(II) removal from kaolinite by electrokinetics, J. Geotech. Eng. 117 (1991) 241–271.
[38] D.D. Runnells, J.L. Larson, A laboratory study of electromigration as a possible field technique for the removal of contaminants from ground water, Ground Water Monit. Rev. 6 (1986) 85.
[39] Y. Katayama, S. Zen, F. Horide, S. Tsuda, K. Tsuji, Effect of surfactants on suspendibility of kaolinite clay and diatomaceous earth in aqueous suspension, Pestic. Sci. 17 (1992) 1–5.
[40] A. Delgado, F. Gonzalez-Caballero, J.M. Bruque, On the zeta potential and surface charge density of montmorillonite in aqueous electrolyte solutions, J. Colloid Interface Sci. 113 (1986) 203–211.
[41] A. Cremers, Surface conductivity in sodium clays, Isr. J. Chem. 6 (1968) 195–202.
[42] V.S. Gupta, S.K. Bhattacharjya, B.K. Dutta, Zeta-potential control for alum coagulation, J. Am. Water Works Assoc. 67 (1975) 21–23.
[43] Y.E. Collins, G. Stotzky, Heavy metals alter the electrokinetic properties of bacteria, yeasts, and clay minerals , Appl. Environ. Microbiol. 58 (1992) 1592–1600.
[44] C.W. Angie, H.A. Hamza, An electrokinetic study of a natural coal associated mixture of kaolinite and montmorillonite in electrolytes, Appl. Clay Sci. 4 (1989) 263–278.
[45] P.B. Lorenz, Surface conductance and electrokinetic properties of kaolinite beds, Clays Clay Miner. 17 (1969) 223–231.
[46] J.K. Wittle, S. Pamukcu, Electrokinetic treatment of contaminated soils, sludges, and lagoons, Final report under Argonne National Laboratory Contract No. 02112406, 1993, DOE formal report.
[47] R.N. Yong, D. Mourato, Influence of polysaccharides on kaolinte structure and properties in a kaolinite–water system, Can. Geotech. J. 27 (1990) 774–788.
[48] R.N. Yong, M. Ohtsubo, Interparticle action and rheology of kaolinite-amorphous iron hydroxide (ferrihydrite) complexes, Appl. Clay Sci. 2 (1987) 63–81.
[49] D.H. Gray, J. Schlocker, Electrochemical alteration of clay soils, Clays Clay Miner. 17 (1969) 309–322.
[50] A. Klute (Ed.), Methods of Soil Analyis: Part 1 — Physical and Mineralogical Methods, 2nd ed., Soil Science Society of America, 1986.